ACS OMEGA

Article

Cite This: ACS Omega 2019, 4, 14100−14104

http://pubs.acs.org/journal/acsodf

Hydrogenated Borophene Shows Catalytic Activity as Solid Acid

Asahi Fujino,[†] Shin-ichi Ito,[‡,∥] Taiga Goto,[†] Ryota Ishibiki,[†] Junko N. Kondo,[⊥] Tadahiro Fujitani,[‡,#] Junji Nakamura,[‡,§] Hideo Hosono,[∥] and Takahiro Kondo*[,‡,§,∥]

[†]Graduate School of Pure and Applied Sciences, [‡]Department of Materials Science, Faculty of Pure and Applied Sciences, and [§]Tsukuba Research Center for Energy Materials Science, University of Tsukuba, 1-1-1, Tennodai, Tsukuba, Ibaraki 305-8573, Japan

[∥]Materials Research Center for Element Strategy, Tokyo Institute of Technology, Yokohama, Kanagawa 226-8503, Japan

[⊥]Institute of Innovative Research, Tokyo Institute of Technology, 4259 Nagatsuta, Yokohama, Kanagawa 226-8503, Japan

[#]Interdisciplinary Research Center, National Institute of Advanced Industrial Science and Technology, 1-1-1 Higashi, Tsukuba, Ibaraki 305-8565, Japan

Supporting Information

ABSTRACT: Hydrogen boride (HB) or hydrogenated borophene sheets are recently realized two-dimensional materials that are composed of only two light elements, boron and hydrogen. However, their catalytic activity has not been experimentally analyzed. Herein, we report the catalytic activity of HB sheets in ethanol reforming. HB sheets catalyze the conversion of ethanol to ethylene and water above 493 K with high selectivity, independent of the contact time, and with an apparent activation energy of 102.8 ± 5.5 kJ/mol. Hence, we identify that HB sheets act as solid-acid catalysts.

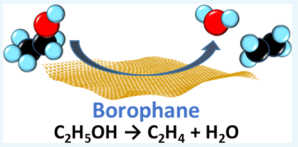

INTRODUCTION

Two-dimensional (2D) materials have great potential for application as catalysts because of their unique properties such as large surface areas and novel electronic states.[1,2] Among 2D materials, boron-related materials have unique characteristics different from other 2D materials in that they have polymorphisms,[3−5] i.e., there are a wide variety of stable 2D phases owing to the capability to form multicenter bonding configurations of boron.[6] Single monoatomic 2D boron (borophene) layers have been fabricated on solid surfaces with several different stable structures,[7] which is consistent with theoretical predictions regarding polymorphs of borophene.[8−10]

These polymorph characteristics of 2D boron sheets provide an opportunity to optimize the catalytic performance by tuning the bonding configurations of the 2D boron network. For example, it has been recently reported that boron nanosheets exfoliated from bulk boron exhibited efficient electrocatalytic performance for NH_3 formation from N_2 in neutral media.[11] Recent experimental and theoretical studies also showed that α-phase molybdenum diboride (α-MoB_2) comprising noble metal-free borophene subunits exhibits superefficient electrocatalytic properties for the hydrogen evolution reaction.[12] What we expect here is that these observed catalytic performances will be further improved by optimizing the electronic structure of 2D boron sheets through the adjusting of the 2D boron bonding-network configurations as well as conventional doping and/or composite formation.

This catalyst design concept with an attractive polymorph 2D boron character can be extended to hydrogenated borophene (referred to as borophane) sheets, since the polymorph 2D phases of borophane have been theoretically predicted.[5] However, the catalytic performance of borophane has not been experimentally analyzed, to the best of our knowledge.

Recently, we revealed that a type of borophane sheet, the hydrogen boride (HB) sheet, with an empirical formula of H_1B_1, can be experimentally prepared by exfoliation and complete ion-exchange between protons and magnesium cations in magnesium diboride (MgB_2), with an average yield of 42.3% at room temperature.[13] Our extensive analysis revealed that the prepared HB sheets did not show any long-range order but have a local structure of a hexagonal boron network with bridge hydrogens, as shown in Figure 1a.[13] A recent analysis using soft X-ray absorption and emission spectroscopy at the B K-shell also supports this view and shows the semimetallicity of HB sheets.[14] HB sheets release their hydrogen content as H_2 molecules in a wide temperature range from 423 to 1473 K.[13] The hydrogen in HB has a character of protons (H^+) rather than that of hydrides (H^-), based on the B 1s core-level states, density functional theory calculations, and the Hammett acidity function (H_0, acid strength); the H_0 of HB sheets is below 1.5 and above 0.43.[13] From this viewpoint, we can regard HB sheets as proton-covered 2D boron sheets. We can thus expect that HB sheets would exhibit intriguing catalytic performance for proton-related chemical reactions and would be used as theoretically predicted hydrogen-storage materials[15,16] and in batteries.[17−19] In this work, we therefore examined the catalytic activity of HB sheets in the ethanol-reforming reaction to clarify their acid/base catalytic property and performance.

Received: July 2, 2019
Accepted: August 1, 2019
Published: August 15, 2019

DOI: 10.1021/acsomega.9b02020
ACS Omega 2019, 4, 14100−14104

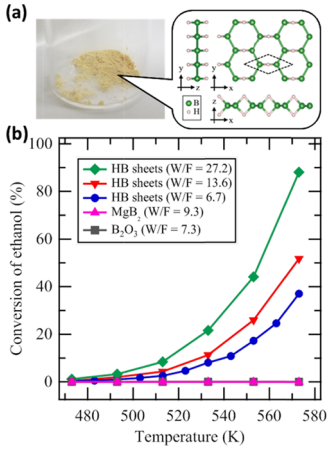

Figure 1. (a) Photograph of HB sheets in powder form and schematic of the proposed local structure.[13] (b) Conversion of ethanol vs temperature. The results for HB, B_2O_3, and MgB_2 are plotted for various W/F (g·min/mmol) conditions (contact time, weight of the catalyst divided by the flow rate of C_2H_5OH).

RESULTS AND DISCUSSION

Figure 1b shows the conversion of ethanol as a function of temperature at various W/F conditions (contact time); W/F (g·min/mmol) is the weight of the catalyst (g) divided by the flow rate of C_2H_5OH (mmol/min). The conversion was estimated from the total amount of hydrocarbons in the product (see the details in the Supporting Information). In every case, we heated the sample at 573 K under Ar flow for 1 h prior to the measurement. It is clear that HB sheets exhibit distinct ethanol conversion, whereas MgB_2 (starting material for the synthesis of HB) and B_2O_3 (product obtained by heating $B(OH)_3$, which is a byproduct in HB sheet synthesis, to 400 K or more) exhibit no ethanol conversion. The conversion by the HB sheets increases with an increase in W/F; it is 90% at 573 K and W/F = 27.2 g·min/mmol. The conversion remains constant for a long period. As an example, the conversion at 573 K and W/F = 7.3 g·min/mmol as a function of the reaction time is shown by blue circles in Figure 2a. In this case, the total amount of hydrocarbons at 13.4 h is 3.2 mmol, which is approximately half of the total B atom numbers of used HB sheets. We also estimated the conversion from the ethanol consumption, as shown by the red triangles in Figure 2a (see the details in the Supporting Information). The conversion calculated from the hydrocarbon production and that from the ethanol consumption are almost the same at 12 h (approximately 40%), indicating that the product hydrocarbon does not accumulate on the catalyst HB sheets during the steady-state catalytic process. These results hence indicate that the HB sheets catalytically convert ethanol. It is notable that pretreatment heating at 573 K causes inevitable hydrogen release from HB as H_2.[13] The maximum amount of released hydrogen at 573 K could be estimated as approximately 33−50 atom % of HB based on the thermal desorption spectroscopy (TDS) results[13] (see the details in the Supporting Information). It is implying that the stoichiometry of the HB sheets showing the catalytic activity was not H:B = 1:1 but approximately H:B = 1:2.5 ± 0.5 (if they were forming a uniform structure).

We detected the catalytically converted products using gas chromatography; they were predominantly ethylene and water, together with other products such as methane, ethane, and a

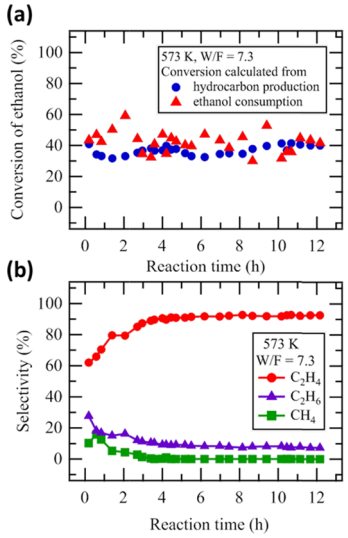

Figure 2. (a) Conversion of ethanol on HB sheets as a function of reaction time at 573 K and W/F = 7.3 g·min/mmol, estimated from hydrocarbon production (blue circles) and ethanol consumption (red triangles). (b) Selectivity vs reaction time.

trace amount of acetaldehyde, as shown in Figure 2b. The selectivity of ethylene was relatively low at the early stage, i.e., 0−4 h reaction time; this could be ascribed to the presence of surplus hydrogen in HB compared with the amount of hydrogen at the steady-state in HB at 573 K (details in the Supporting Information). We observed the same characteristics at all of the measured temperatures and W/F conditions, as shown in Figure 3a,b; i.e., C_2H_4 was always the main

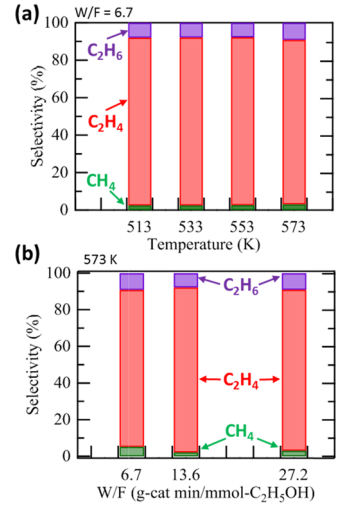

Figure 3. (a) Selectivity of ethanol reforming by HB as a function of temperature at W/F = 6.7 g·min/mmol. (b) Selectivity of ethanol reforming by HB at 573 K and W/F = 6.7, 13.6, and 27.2 g·min/mmol.

product, and the selectivity for the obtained total hydrocarbon was almost the same. These results indicate that the major catalytic reaction of ethanol reforming by the HB sheets is the dehydration reaction: $C_2H_5OH \rightarrow C_2H_4 + H_2O$. It is known that if a catalyst promotes the dehydration reaction of ethanol, it is a solid-acid; however, if the dehydrogenation reaction occurs, producing an acetaldehyde, the catalyst is a base catalyst. The HB sheets are therefore solid-acid catalysts, which

DOI: 10.1021/acsomega.9b02020
ACS Omega 2019, 4, 14100−14104

is consistent with the H_0 of the HB sheets (below 1.5 and above 0.43)[13] in terms of the acidic character.

Figure 4 shows the Arrhenius plot of the ethanol-reforming reaction rate k, which was calculated by assuming a first-order

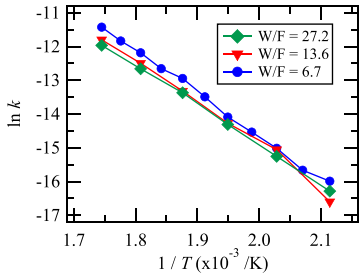

Figure 4. Arrhenius plot of the ethanol-reforming reaction rate (k) in the presence of HB sheets for W/F = 27.2, 13.6, and 6.7 g·min/mmol.

reaction, as k = (C_2H_5OH conversion [%])/100 × (C_2H_5OH flux [mol/s])/(HB amount [mol]), for the results under various W/F conditions with the HB sheets. As the obtained linear lines are almost the same and they are independent of W/F, the reaction can be (at least apparently) considered a first-order reaction. To determine the exact reaction order and mechanism, further kinetic analysis is required. From the slope and the section, the apparent activation energy E_a and pre-exponential factor A were estimated to be 102.8 ± 5.5 kJ/mol and 3.5×10^4 s^{-1}, respectively. The derived E_a is comparable to the reported activation energies for the catalytic dehydration of ethanol over Al_2O_3 (53−155 kJ/mol),[20,21] the Lewis acidic Zr-KIT-6 catalyst (79 kJ/mol),[22] silica−alumina (125.5 kJ/mol),[23] and microporous Fe-ZSM-5 (137.7−271.1 kJ/mol).[24] The formation rate of ethylene on our HB catalyst at 573 K and W/F = 7.3 g·min/mmol was 2.4 ± 0.1 mmol/g·h (Figure 2). Although this is not the formation rate at the optimal catalytic condition, here, we compare it with those of the other reported catalysts. Chen and co-workers reported that the formation rate of ethylene from ethanol using the commercial SynDol (Al_2O_3−MgO/SiO_2) catalyst was 7.8 mmol/g·h at 591 K, with a weight hourly space velocity (WHSV) of 0.23 h^{-1} in a fixed-bed reactor (this value is calculated using the reported yield of the ethylene, which is 0.22 g/gcat·h).[25] They also reported a higher formation rate of 535 mmol/g·h on Ti/γ-Al_2O_3 at 633 K and WHSV of 26 h^{-1} using the microreactor (calculated using a value of 15 g/gcat·h).[25] The formation rate of HB sheets is, thus, lower than that of the state-of-the-art catalysts but is in the same order as that of the commercial SynDol catalyst.

Finally, we herein discuss the possible reaction mechanism and active sites as well as the acid property of the HB sheets. In the case of ethanol reforming on a zeolite catalyst,[26−32] diethyl ether ($C_2H_5OC_2H_5$) is formed as a result of a two-molecule reaction. Diethyl ether then converts to ethylene at strong Brønsted acid sites. The number and the strength of strong Brønsted acid sites in the catalyst are thus reported to determine the catalytic activity for ethylene formation. Since HB sheets show weaker H_0 ($1.5 \geq H_0 \geq 0.43$)[13] compared with that of zeolites (e.g., $-3.0 \geq H_0 \geq -8.2$ of H-Zeolite),[33] we can expect the formation of diethyl ether rather than ethylene on HB sheets, based on the trend of zeolite. However, we observed ethylene instead of diethyl ether on the HB sheets (Figures 2 and 3). Thus, the reaction is considered to proceed as a single molecule reaction via the formation of an ethoxy (C_2H_5O-) species rather than the two-molecule reaction via the formation of diethyl ether. Indeed, the derived apparent activation energy (102.8 ± 5.5 kJ/mol) from Figure 4 is similar to that for the decomposition of the ethoxy intermediate generated from ethanol on a zeolite (122 ± 3 kJ/mol).[34] The ethoxy species can thus be formed prior to ethylene on HB; this will be investigated using infrared spectroscopy in our future work. Concerning the active site, the bridge-type hydrogen in the HB sheets and/or terminal-type hydrogen at the edge of the HB sheets can be expected to act as the Brønsted acid sites. However, as described above, the stoichiometry of the HB sheets used in this work for the catalytic activity measurements is not H:B = 1:1 due to the inevitable hydrogen release as H_2 at the pretreatment heating of 573 K (release as much as 33−50% of hydrogen in HB). Thus, we cannot simply assign the hydrogen atoms of the outermost surface (bridge- and/or edge-type of hydrogens) of HB (Figure 1a) as the active sites. There is a possibility that the boron atom that does not bond with hydrogen acts as the Lewis acid site if a hydrogen vacancy is created locally and the boron atom adopts a simple sp^2 bonding configuration with surrounding boron atoms (Figure 1a) without any electron in its p_z orbital. On the other hand, if the charges in the HB sheets are delocalized well to supply electrons to the p_z orbital of a bare sp^2-bonded boron atom (at hydrogen vacancy), the boron atom may act as a Brønsted base, similar to the lattice oxygen in zeolite, and promote the dehydrogenation of ethoxy to form ethylene. According to our catalytic activity measurements for the HB sheets without pretreatment heating (Figure S4), the selectivity is different from that shown in Figure 3. This difference in selectivity can be attributed to the difference in the hydrogen amount in HB, as in the case of the origin of the induction period shown in Figure 2b (see the details in the Supporting Information). We can hence at least classify that the HB and heated HB (hydrogen-deficient-HB) have different catalytic properties (i.e., different acid sites). However, the active sites cannot be solely determined by our current experimental results. At least it should be clarified whether the hydrogen-deficient HB consists of a uniform stoichiometric structure or defective structure. Further investigation is thus required to determine the exact active sites of the HB solid-acid catalyst, e.g., the careful structure characterization, infrared spectroscopy analysis with pyridine, NH_3, and CO_2 adsorption, and H_0 measurements with quantitative density, as a function of the pretreatment heating temperature (i.e., hydrogen amount in HB).

■ CONCLUSIONS

We found that hydrogen boride or hydrogenated borophene sheets catalyze the conversion of ethanol to ethylene and water above 493 K, with high selectivity, independent of the contact time, and an apparent activation energy of 102.8 ± 5.5 kJ/mol. We hence consider hydrogenated borophene sheets to be novel, nonmetal, and two-dimensional solid-acid catalysts that have great potential for application as hydrogen-storage materials and in batteries.

■ EXPERIMENTAL SECTION

Materials. HB sheets were prepared using a previously reported ion-exchange method.[13] Specifically, MgB_2 powder (1.0 g, 99%, Rare Metallic Co., Ltd., Tokyo, Japan) in acetonitrile (300 mL, 99.5%, Wako Pure Chemical Industries

DOI: 10.1021/acsomega.9b02020
ACS Omega 2019, 4, 14100−14104

Ltd., Osaka, Japan) was mixed with a solution of an ion-exchange resin (60 mL, Amberlite IR120B hydrogen form, Organo Corp., Tokyo, Japan) and acetonitrile (200 mL) in a Schlenk flask under a nitrogen atmosphere, where water inclusion is sensitive to the product[35] and thus careful removal of water was done beforehand. This mixture was stirred using a magnetic stirrer at 400 rpm for 2 days at room temperature. The supernatant was then kept for 1 day at 255 K to physically separate the byproduct $B(OH)_3$. Dried HB sheets were prepared by heating the resulting liquid at 343 K while pumping with a liquid nitrogen trap. For all of the syntheses, we carefully confirmed the product by X-ray photoelectron spectroscopy to confirm the absence of Mg and the presence of negatively charged B without oxidized B as reported previously.[13] Moreover, we recently confirmed using atomic force microscopy (AFM) that our HB sheets mostly consist of a few to several tens of layers. The details of AFM with statistical analysis will be published in our future work.

Catalytic Activity Measurements. To determine the catalytic activity, gaseous ethanol was introduced into the HB sheets using an argon carrier gas under atmospheric pressure in a homemade fixed-bed flow reactor. The product gas was then analyzed using a thermal conductivity detector in a gas chromatograph (GC-8A, Shimadzu, Kyoto, Japan) equipped with Molecular Sieve 5A and Porapak Q at the downstream end of the reactor. The catalytic conversion was estimated from the total amount of hydrocarbon production using the following relation

$$\text{ethanol conversion (\%)} = [(\text{number of total carbon in detected hydrocarbon molecules})(\text{mol/min})] / [\text{introduced ethanol molecules} \times 2\ (\text{mol/min})] \times 100$$

As shown in Figure 2a, the conversion was also estimated from ethanol consumption as follows

$$\text{ethanol conversion (\%)} = [(\text{introduced ethanol molecules} - \text{detected ethanol molecules})\ (\text{mol/min})] / [\text{introduced ethanol molecules (mol/min)}] \times 100$$

The selectivity was estimated using the following relation

$$\text{selectivity of specific product (\%)} = \frac{\text{total amount of specific product (mol)}}{\text{total amount of products (mol)}} \times 100$$

The catalytic activity was determined under various W/F conditions (g·min/mmol), which is the weight of the catalyst (g) divided by the flow rate of C_2H_5OH (mmol/min); W/F was controlled by adjusting the flow rate of C_2H_5OH and the weight of the sample. The W/F conditions used in this work are listed in Table S1.

■ ASSOCIATED CONTENT

Supporting Information

The Supporting Information is available free of charge on the ACS Publications website at DOI: 10.1021/acsomega.9b02020.

Origin of the induction period, TDS, effect of water, and catalytic activity of HB without pretreatment heating (PDF)

■ AUTHOR INFORMATION

Corresponding Author

*E-mail: takahiro@ims.tsukuba.ac.jp.

ORCID

Junko N. Kondo: 0000-0002-7940-1266
Tadahiro Fujitani: 0000-0002-1225-3246
Hideo Hosono: 0000-0001-9260-6728
Takahiro Kondo: 0000-0001-8457-9387

Notes

The authors declare no competing financial interest.

■ ACKNOWLEDGMENTS

This work was supported by the JSPS KAKENHI nos. JP 18K18989, JP 19H05046, and JP 19H02551 and Murata Science Foundation, KUMAGAI, Ogasawara, and Samco foundations for the Promotion of Science & Engineering. T.K., S.-i.I., and H.H. were supported by the MEXT Element Strategy Initiative to Form Core Research Center.

■ REFERENCES

(1) Wang, Y.; Mao, J.; Meng, X.; Yu, L.; Deng, D.; Bao, X. Catalysis with Two-Dimensional Materials Confining Single Atoms: Concept, Design, and Applications. *Chem. Rev.* **2019**, *119*, 1806−1854.

(2) Deng, D.; Novoselov, K. S.; Fu, Q.; Zheng, N.; Tian, Z.; Bao, X. Catalysis with Two-Dimensional Materials and Their Heterostructures. *Nat. Nanotechnol.* **2016**, *11*, 218−230.

(3) Zhang, Z.; Penev, E. S.; Yakobson, B. I. Two-Dimensional Boron: Structures, Properties and Applications. *Chem. Soc. Rev.* **2017**, *46*, 6746−6763.

(4) Kondo, T. Recent Progress in Boron Nanomaterials. *Sci. Technol. Adv. Mater.* **2017**, *18*, 780−804.

(5) Jiao, Y.; Ma, F.; Bell, L.; Bilic, A.; Du, A. Two-Dimensional Boron Hydride Sheets:High Stability, Massless Dirac Fermions, and Excellent Mechanical Properties. *Angew. Chem. Int. Ed.* **2016**, *55*, 10292−10295.

(6) Oganov, A. R.; Solozhenko, V. L. Boron: A Hunt for Superhard Polymorphs. *J. Superhard Mater.* **2009**, *31*, 285−291.

(7) Mannix, A. J.; Kiraly, B.; Hersam, M. C.; Guisinger, N. P. Synthesis and Chemistry of Elemental 2D Materials. *Nat. Rev. Chem.* **2017**, *1*, 0014.

(8) Boustani, I. New Quasi-Planar Surfaces of Bare Boron. *Surf. Sci.* **1997**, *370*, 355−363.

(9) Penev, E. S.; Bhowmick, S.; Sadrzadeh, A.; Yakobson, B. I. Polymorphism of Two-Dimensional Boron. *Nano Lett.* **2012**, *12*, 2441−2445.

(10) Wu, X.; Dai, J.; Zhao, Y.; Zhuo, Z.; Yang, J.; Zeng, X. C. Two-Dimensional Boron Monolayer Sheets. *ACS Nano* **2012**, *6*, 7443−7453.

(11) Zhang, X.; Wu, T.; Wang, H.; Zhao, R.; Chen, H.; Wang, T.; Wei, P.; Luo, Y.; Zhang, Y.; Sun, X. Boron Nanosheet: An Elemental Two-Dimensional (2D) Material for Ambient Electrocatalytic N_2 -to-NH_3 Fixation in Neutral Media. *ACS Catal.* **2019**, *9*, 4609−4615.

(12) Chen, Y.; Yu, G.; Chen, W.; Liu, Y.; Li, G.; Zhu, P.; Tao, Q.; Li, Q.; Liu, J.; Shen, X.; et al. Highly Active, Nonprecious Electrocatalyst Comprising Borophene Subunits for the Hydrogen Evolution Reaction. *J. Am. Chem. Soc.* **2017**, *139*, 12370−12373.

(13) Nishino, H.; Fujita, T.; Cuong, N. T.; Tominaka, S.; Miyauchi, M.; Iimura, S.; Hirata, A.; Umezawa, N.; Okada, S.; Nishibori, E.; et al. Formation and Characterization of Hydrogen Boride Sheets Derived from MgB_2 by Cation Exchange. *J. Am. Chem. Soc.* **2017**, *139*, 13761−13769.

(14) Tateishi, I.; Cuong, N. T.; Moura, C. A. S.; Cameau, M.; Ishibiki, R.; Fujino, A.; Okada, S.; Yamamoto, A.; Araki, M.; Ito, S.; et al. Semimetallicity of Free-Standing Hydrogenated Monolayer Boron from MgB_2. *Phys. Rev. Mater.* **2019**, *3*, No. 024004.

DOI: 10.1021/acsomega.9b02020
ACS Omega 2019, 4, 14100−14104

(15) Chen, L.; Chen, X.; Duan, C.; Huang, Y.; Zhang, Q.; Xiao, B. Reversible Hydrogen Storage in Pristine and Li Decorated 2D Boron Hydride. *Phys. Chem. Chem. Phys.* **2018**, *20*, 30304−30311.
(16) Abtew, T. A.; Shih, B. C.; Dev, P.; Crespi, V. H.; Zhang, P. Prediction of a Multicenter-Bonded Solid Boron Hydride for Hydrogen Storage. *Phys. Rev. B: Condens. Matter Mater. Phys.* **2011**, *83*, No. 094108.
(17) Makaremi, M.; Mortazavi, B.; Singh, C. V. 2D Hydrogenated Graphene-like Borophene as a High Capacity Anode Material for Improved Li/Na Ion Batteries: A First Principles Study. *Mater. Today Energy* **2018**, *8*, 22−28.
(18) Xiang, P.; Chen, X.; Xiao, B.; Wang, Z. M. Highly Flexible Hydrogen Boride Monolayers as Potassium-Ion Battery Anodes for Wearable Electronics. *ACS Appl. Mater. Interfaces* **2019**, *11*, 8115−8125.
(19) Shukla, V.; Araujo, R. B.; Jena, N. K.; Ahuja, R. Borophene's Tryst with Stability: Exploring 2D Hydrogen Boride as an Electrode for Rechargeable Batteries. *Phys. Chem. Chem. Phys.* **2018**, *20*, 22008−22016.
(20) Bakoyannakis, D. N.; Zamboulis, D.; Stalidis, G. A.; Deliyanni, E. A. The Effect of Preparation Method on the Catalytic Activity of Amorphous Aluminas in Ethanol Dehydration. *J. Chem. Technol. Biotechnol.* **2001**, *76*, 1159−1164.
(21) Christiansen, M. A.; Mpourmpakis, G.; Vlachos, D. G. Density Functional Theory-Computed Mechanisms of Ethylene and Diethyl Ether Formation from Ethanol on γ-Al_2O_3(100). *ACS Catal.* **2013**, *3*, 1965−1975.
(22) Pan, Q.; Ramanathan, A.; Kirk Snavely, W.; Chaudhari, R. V.; Subramaniam, B. Intrinsic Kinetics of Ethanol Dehydration over Lewis Acidic Ordered Mesoporous Silicate, Zr-KIT-6. *Top. Catal.* **2014**, *57*, 1407−1411.
(23) Roca, F.; De Mourgues, L.; Trambouze, Y. Catalytic Dehydration of Ethanol over Silica-Alumina. *J. Catal.* **1969**, *14*, 107−113.
(24) Maihom, T.; Khongpracha, P.; Sirijaraensre, J.; Limtrakul, J. Mechanistic Studies on the Transformation of Ethanol into Ethene over Fe-ZSM-5 Zeolite. *ChemPhysChem* **2013**, *14*, 101−107.
(25) Chen, G.; Li, S.; Jiao, F.; Yuan, Q. Catalytic Dehydration of Bioethanol to Ethylene over TiO_2/γ-Al_2O_3 Catalysts in Microchannel Reactors. *Catal. Today* **2007**, *125*, 111−119.
(26) Takahara, I.; Saito, M.; Inaba, M.; Murata, K. Dehydration of Ethanol into Ethylene over Solid Acid Catalysts. *Catal. Lett.* **2005**, *105*, 249−252.
(27) Madeira, F. F.; Gnep, N. S.; Magnoux, P.; Maury, S.; Cadran, N. Ethanol Transformation over HFAU, HBEA and HMFI Zeolites Presenting Similar Brønsted Acidity. *Appl. Catal., A* **2009**, *367*, 39−46.
(28) Chiang, H.; Bhan, A. Catalytic Consequences of Hydroxyl Group Location on the Rate and Mechanism of Parallel Dehydration Reactions of Ethanol over Acidic Zeolites. *J. Catal.* **2010**, *271*, 251−261.
(29) Xin, H.; Li, X.; Fang, Y.; Yi, X.; Hu, W.; Chu, Y.; Zhang, F.; Zheng, A.; Zhang, H.; Li, X. Catalytic Dehydration of Ethanol over Post-Treated ZSM-5 Zeolites. *J. Catal.* **2014**, *312*, 204−215.
(30) Kadam, S. A.; Shamzhy, M. V. IR Operando Study of Ethanol Dehydration over MFI Zeolites. *Catal. Today* **2018**, *304*, 51−57.
(31) Zhang, M.; Yu, Y. Dehydration of Ethanol to Ethylene. *Ind. Eng. Chem. Res.* **2013**, *52*, 9505−9514.
(32) Sun, J.; Wang, Y. Recent Advances in Catalytic Conversion of Ethanol to Chemicals. *ACS Catal.* **2014**, *4*, 1078−1090.
(33) Varvarin, A. M.; Khomenko, K. M.; Brei, V. V. Conversion of N-Butanol to Hydrocarbons over H-ZSM-5, H-ZSM-11, H-L and H-Y Zeolites. *Fuel* **2013**, *106*, 617−620.
(34) Kondo, J. N.; Yamazaki, H.; Osuga, R.; Yokoi, T.; Tatsumi, T. Mechanism of Decomposition of Surface Ethoxy Species to Ethene and Acidic OH Groups on H-ZSM-5. *J. Phys. Chem. Lett.* **2015**, *6*, 2243−2246.
(35) Nishino, H.; Fujita, T.; Yamamoto, A.; Fujimori, T.; Fujino, A.; Ito, S.; Nakamura, J.; Hosono, H.; Kondo, T. Formation Mechanism of Boron-Based Nanosheet through the Reaction of MgB_2 with Water. *J. Phys. Chem. C* **2017**, *121*, 10587−10593.

NOTE ADDED AFTER ASAP PUBLICATION

This paper published ASAP on August 15, 2019 with an inaccurate equation due to production error. The corrected version reposted to the Web on August 19, 2019.

DOI: 10.1021/acsomega.9b02020
ACS Omega 2019, 4, 14100−14104